Environ Earth Sci (2016) 75:1472
DOI 10.1007/s12665-016-6275-0

ORIGINAL ARTICLE

Effects of intertidal reclamation on tides and potential environmental risks: a numerical study for the southern Yellow Sea

Qingguang Zhu[1,2] · Ya Ping Wang[1] · Wenfei Ni[3] · Jianhua Gao[1] · Minliang Li[4] · Lei Yang[4] · Xulong Gong[4] · Shu Gao[5]

Received: 28 March 2016 / Accepted: 16 November 2016 / Published online: 25 November 2016

Abstract Intertidal (tidal flat) reclamation along the Chinese coastline, especially which is in Jiangsu Province, has increased markedly in recent years. However, the hydrodynamic disturbance and environmental impacts of this activity are not yet fully understood. In this study, a process-based depth-averaged model is used to evaluate quantitatively the possible impacts of intertidal reclamation for the southern Yellow Sea region. The simulation results show that reclamation of both inshore and offshore intertidal areas of $\sim$1800 km^2 (according to the approved governmental reclamation scheme) would result in three remarkable changes in tidal patterns: enhanced M_2 and M_4 tidal amplitudes in coastal areas, strengthened negative tidal asymmetry in the southern region of the sand ridge system, and an enhanced tidal energy flux toward offshore through the main channels in the south. These changes would result in some negative impacts. The enhancement in local tidal amplitude could increase the probability of coastal hazards, and the offshore sediment transport tendency resulting from negative tidal asymmetry in the south could lead to severe erosion. The enhanced energy flux transported offshore may also affect far-field regions. On the other hand, alternative reclamation of $\sim$400 km^2 of offshore intertidal area could significantly minimize hydrodynamic disturbances to the local tidal system. Offshore reclamation with lower environment impacts may be the future for coastal development. To cope with the potential environmental risks caused by reclamation, it is recommended to strengthen environmental impact assessment and overseeing of reclamation plans, and advance international cooperation in terms of coastal management. Our findings provide a reference for coastal management in countries with substantial areas of tidal flats.

Keywords Tidal dynamics · Intertidal area · Reclamation · Numerical modeling · The southern Yellow Sea

✉ Ya Ping Wang
ypwang@nju.edu.cn

[1] School of Geographic and Oceanographic Sciences, Nanjing University, Nanjing 210023, Jiangsu, China

[2] Key Laboratory of the Coastal Zone Exploitation and Protection, Ministry of Land and Resource, Nanjing, China

[3] Center for Environmental Science, University of Maryland, Cambridge, MD 21613, USA

[4] Geological Survey of Jiangsu Province, Nanjing 210018, Jiangsu, China

[5] State Key Laboratory for Estuarine and Coastal Studies, East China Normal University, Shanghai 200046, China

Introduction

Tidal current movement is one of the most important hydrodynamic processes in the Yellow Sea, which is characterized by relatively large tidal ranges (3.9–5.5 m) and complex tidal dynamics (Ren 1986). Since the 1980s, the tidal characteristics in this region have been widely investigated by field observations (e.g., Nishida 1980; Larsen et al. 1985; Fang 1986; Kang 1999; Fang et al. 2004) and numerical models (e.g., Guo and Yanagi 1998; Kang et al. 1998; Bao et al. 2001; Xing et al. 2012; Zhu and Liu 2012).

Intertidal areas play an important role in tidal energy storage and dissipation. A reduction in the area of tidal flats (e.g., reclamation of intertidal areas) would affect tidal energy dissipation, which is dominated by friction in shallow water (Song et al. 2013). As a consequence, distortion of astronomical tides in shallow water caused by tidal flats reduction will result in tidal asymmetry and make

a significant impact on sediment transport processes (Nidzieko and Ralston 2012; Ralston et al. 2013).

Although intertidal reclamation can yield enormous economic benefits, it changes the local hydrodynamics (Camorani et al. 2005; Jiao et al. 2006; Li et al. 2012) and results in pollution due to the release of reclamation materials (Chen and Jiao 2008; Naser 2011), wetland losses (Cho 2007; Fernández et al. 2010), and changes of erosion and siltation patterns (Wang et al. 2012b; Li et al. 2014). Large-scale intertidal reclamation has both local and far-field effects on tidal dynamics (Song et al. 2013).

For the purpose to resolve the land shortage as cities and industries expand, coastal land reclamation in China has increased rapidly, especially in Jiangsu Province. Located on the coastal plain of the southern Yellow Sea, the province has a long history of land reclamation; over the last 100 years, some 6360 km^2 of tidal flats has been reclaimed (Fig. 1). The explosions in 1910s and 1950s were due to large-scale cotton cultivation and saltern expansion, respectively, in the special historical periods of Chinese modernization (Zhang et al. 2013). In recent decades, the reclamation area in Jiangsu increased significantly with the promotion of reclamation projects. Following sequential reclamation, the grain size of surficial sediment had a finer tendency on the mid-upper intertidal flat but a coarser tendency on the lower intertidal flat, in response to a reduction in the tidal current speed over the intertidal zone and the aggrandizement of wave action over the lower intertidal flat (Wang et al. 2012b).

Recently, a major land reclamation scheme on the Jiangsu coast, covering an area of 1800 km^2, will be implemented by 2020 (Jiangsu Development and Reform Commission and Jiangsu Coastal Areas Development Office 2009). The reclamation area of this

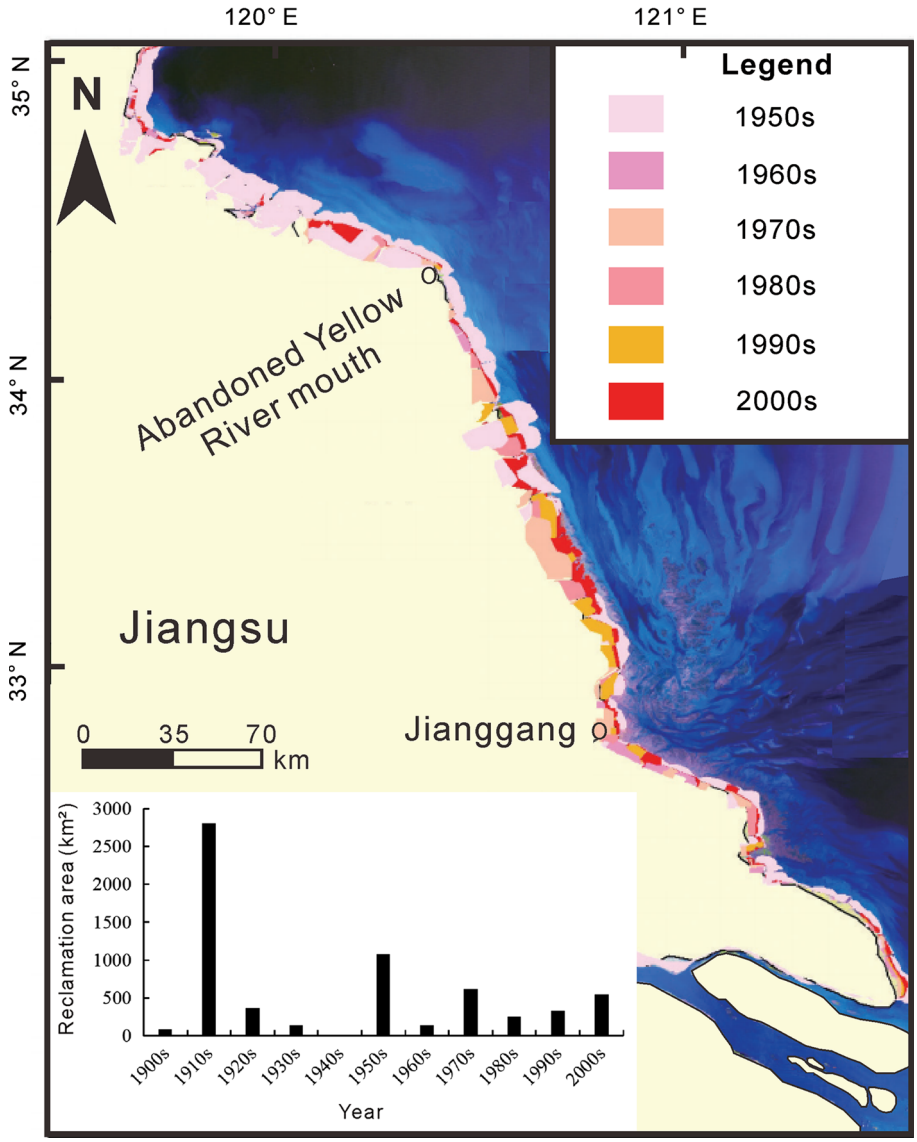

Fig. 1 Land reclamation history of Jiangsu Province. Modified from Zhang et al. (2013)

scheme occupies 30.6% of the overall coastal reclamation demand by respective Chinese provinces and metropolises by 2020 (Wang et al. 2014). Nevertheless, how this unique large-scale intertidal reclamation project will impact the local environment remains unknown. As summarized by Wang et al. (2014), China's land reclamation in recent decades has resulted in reduction of coastal wetland areas, decline of ecosystem service value of coastal wetlands, destruction of coastal landscape diversity, and decline in coastal disaster prevention capacity. This paper serves as a further study of Wang et al. (2014) to investigate the effects of intertidal reclamation on tides and potential environmental risks caused by the imminent reclamation project in Jiangsu. Based upon our simulation results, some mitigating measures and management strategies to cope with the possible environmental impacts are recommended.

Regional setting

Our study focuses on the coastal area of the southern Yellow Sea, which is situated between the Changjiang River estuary and the abandoned Yellow River mouth (Fig. 2a). A large offshore radial tidal ridge system consists of ~70 sand ridges in water depths of 20–30 m and converges at Jianggang city (Liu et al. 1989; Fig. 2b). This sand ridge system is 90 km wide in an east–west direction and 200 km long in a northwest–southeast direction (Wang et al. 2012a). Along the coast of Jiangsu, the Yellow Sea Coastal Current (also named as the Subei Longshore Current) flows southward to the Changjiang River mouth (Fig. 2a). Meanwhile, the prominent Changjiang River longshore current extends from the Changjiang offshore to the southeast Zhejiang and Fujian coasts (Wang et al. 2007).

Tidal flats in this region cover an area of 5000 km^2 (Zhang 2011). Partially sheltered by the radial ridge system off the Jiangsu coast, they consist of fine-grained sediment sourced from the ridge system, the abandoned Yellow River delta, and the Changjiang River (Wang et al. 2012b). This region has a semidiurnal tidal cycle with a macrotidal range of 3.9–5.5 m (Ren 1986). The East China Sea progressive tidal wave and the southern Yellow Sea rotary tidal wave converge near the Jianggang coast, resulting in a maximum mean tidal range of 5 m, which decreases to the north and south (Zhang 1992). Overall, this region is dominated by the flood currents rather than the ebb currents (Zhang 1992). Under these hydrodynamic conditions, fine-grained sediments have a landward transport tendency, resulting in continuing growth of tidal flats as they

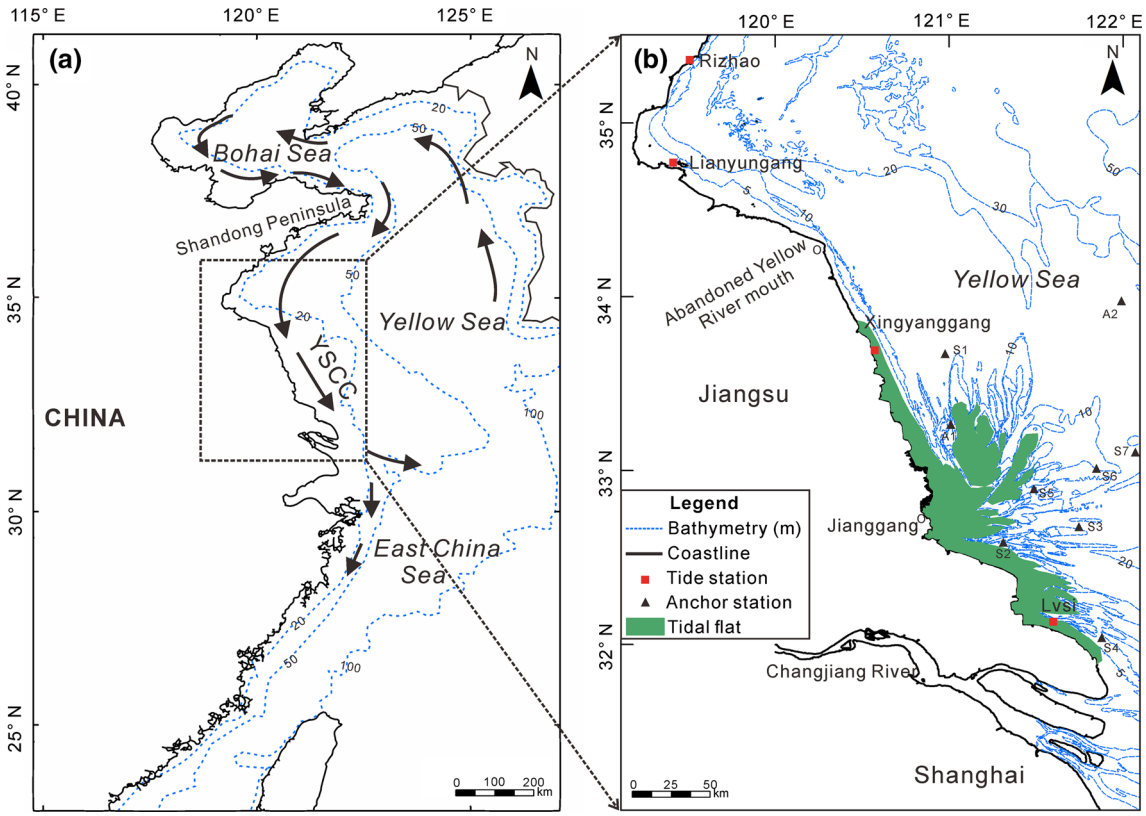

Fig. 2 Maps showing the study area: **a** the Yellow Sea Coastal Current (YSCC) flowing southward along the Jiangsu coast and an overview of the study area; **b** locations of observation stations

accumulate over the intertidal area (Zhang 1992). Surface sediments here are mostly silts and sandy silts (Wang and Ke 1997).

Methodology

Model description

Delft3D, a computational fluid dynamics package, was used to model the hydrodynamic processes in the southern Yellow Sea. It is widely used and has been validated for various coastal environments (Hu et al. 2009; Apotsos et al. 2011; Storlazzi et al. 2011; Leonardi et al. 2013). The continuity equation and nonlinear, shallow-water momentum equations for incompressible free surface flow were discretized on a 3D curvilinear finite difference grid and solved numerically by an alternating direction implicit (ADI) scheme (Edmonds and Slingerland 2007). Further details of this model can be found in Lesser et al. (2004).

Model configuration

Domain

The model domain extends from Shandong Peninsula to the Changjiang River estuary. The southern and eastern boundaries are open oceanic boundaries, and the eastern boundary is ~300 km from the coastline of Jiangsu. The distribution of the 60,000 model-generated curved orthogonal grid cells is shown in Fig. 3. The resolution of grid cells near the coast is ~700 m, while the resolution is ~4600 m in the open sea. Bathymetry data are from detailed marine charts (1:250,000 scale) published in 1995 by the Maritime Safety Administration of P. R. China and adjusted to mean sea level.

Boundary conditions and parameters

Open seaward boundaries were forced with principal tidal constituents (M_2, S_2, K_1, O_1, K_2, M_4, and MS_4) extracted from the southern Yellow Sea model of Xing et al. (2012). The open boundary conditions were specified by data assimilation techniques using TOPEX/Poseidon (T/P) altimeter data and tide gauge station data (Zhang et al. 2011).

Wind is an important driving force influencing hydrodynamic processes and sediment resuspension in coastal areas (Whitney and Garvine 2005). Sensitivity analyses were performed to examine local wind field effects at stations A1 (shallow water) and A2 (deep water) for 2 months during summer and winter, respectively, with and without local wind field (Fig. 4). Wind field data (with a resolution of 25 km) were obtained from ASCAT Ocean Surface Wind Vectors at a height of 10 m (http://manati.star.nesdis.noaa.gov/datasets/ASCATData.php?parname=wv2). The results show that wind has a negligible effect on water level and depth-averaged velocity except under extreme weather conditions. When the wind speed achieves maximum with ~15 m/s, the difference of water level in sensitivity test can reach 0.2 m and the difference of depth-averaged velocity can reach 0.2 m/s. Although extreme weather conditions (the frequency of occurrences is lower than 10%) might cause significant impacts on the hydrodynamic environment in the study area, the dominant factor controlling the hydrodynamics in this region is tidal

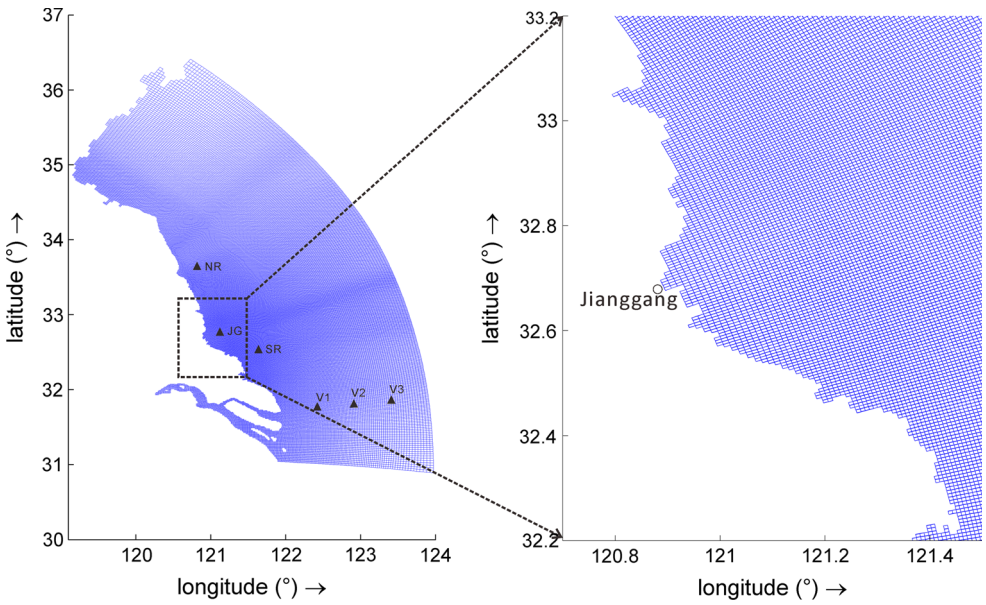

Fig. 3 Model grid cells distribution (stations V1, V2, and V3 are stations for sensitivity analyses of freshwater–saltwater mixing process; stations NR, JG, and SR are stations for comparison of tidal amplitude variation caused by reclamation, which denote the northern region, Jianggang, and the southern region, respectively)

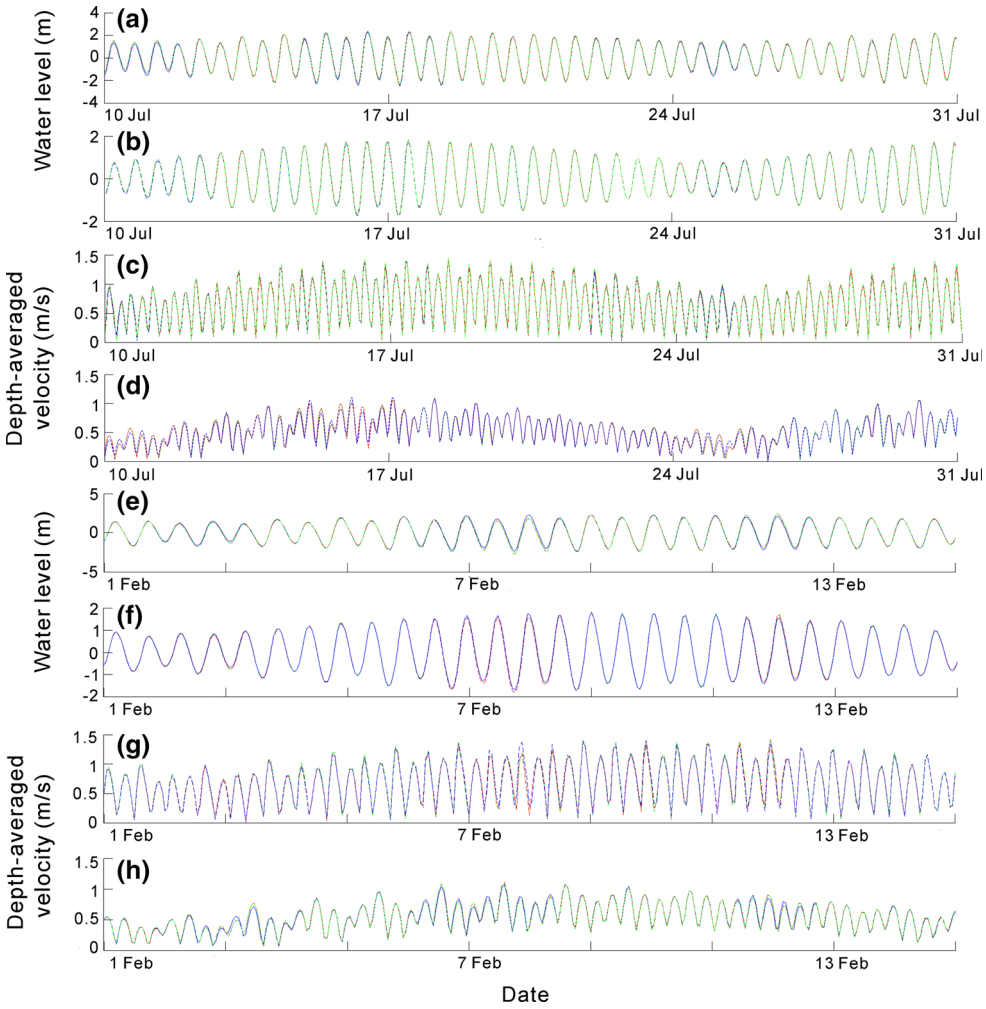

Fig. 4 Sensitivity analyses performed to examine the effects of wind field and depth-averaging on the model simulation: water level in summer **a** A1 and **b** A2; depth-averaged velocity in summer **c** A1 and **d** A2; water level in winter **e** A1 and **f** A2; depth-averaged velocity in winter **g** A1 and **h** A2. *Blue* and *red lines* show simulation results for the 2DH case without and with a local wind field, respectively. *Green lines* show results for a three-dimensional case with a local wind field

currents (Ren 1986). Considering the main goal of our study (to examine the effects of reclamation on tides) and referring to previous modeling studies (Xing et al. 2012), we believe that a model without local wind field could accurately model the general hydrodynamic field in this region. We also conducted sensitivity analyses to evaluate the influence of depth-averaging between a three-dimensional (3D) case and a two-dimensional (2DH) case; the differences were relatively small (Fig. 4).

The study area is in a shallow continental shelf environment. As a result, the salinity has a low gradient with minimal stratification, except for the area near the Changjiang River estuary. We performed sensitivity analyses at stations V1, V2, and V3 (shown in Fig. 3) to evaluate the influence of freshwater–seawater mixing near the Changjiang River estuary. We ran a 3D simulation from June 1, 2011, to January 1, 2012, with 20 vertical layers. Salinity was set to 32 psu and the average monthly freshwater discharge from the Changjiang River was set to 30,980, 42,825, 48,080, 40,930, 26,122, 15,023, and 10,925 m^3/s, respectively, according to the monthly hydrological data recorded by the Datong Hydrological Observation Station of the Changjiang River. We compared the 2DH barotropic simulation without freshwater input with the 3D baroclinic simulation. The comparison result showed a difference in water level of <0.01 m among stations V1, V2, and V3 (Fig. 5). In addition, the difference of depth-averaged velocity between a 2DH barotropic simulation and 3D baroclinic simulation is <0.02 m/s in average (Fig. 6). Considering the strong Subei Longshore Current flowing southward, our sensitivity analyses results indicate that freshwater–seawater mixing in the Changjiang River had a negligible effect on the water level and tidal current movement in our study area. Therefore, we neglected the stratification effect and chose a uniform seawater density of 1025 kg/m^3 for the model. Given the computational efficiency and the dominant role of tidal currents in the study area, we chose to run a 2DH tidal model without the effects of wind, river runoff, and stratification.

To approximate the tidal flat bottom, we use the Manning formula for parameterizing a depth-dependent bottom friction coefficient from Ertürk et al. (2002):

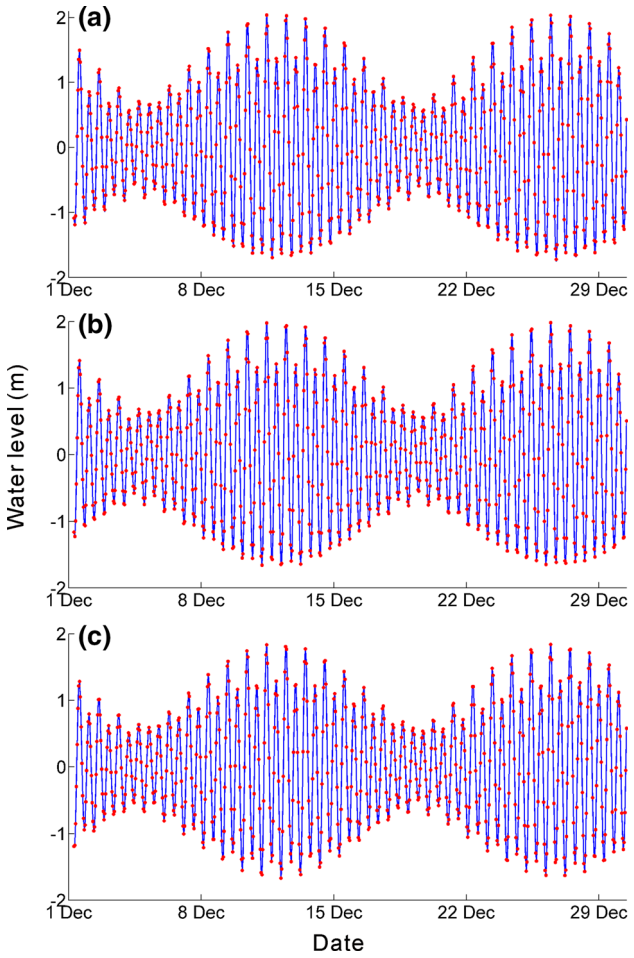

Fig. 5 Comparison of barotropic and baroclinic water level at stations **a** V1; **b** V2; and **c** V3. *Red dots* represent the 3D baroclinic simulation, and *blue lines* show the 2DH barotropic simulation

$$C_{\mathrm{d}} = \frac{gn^2}{H^{\frac{1}{3}}}, \tag{1}$$

$$n = \frac{1}{0.015 + \frac{0.01}{|H|}}, \tag{2}$$

where C_{d} is the bottom drag coefficient ($\mathrm{m}^{4/3}/\mathrm{s}^4$), g is acceleration due to gravity ($\mathrm{m/s}^2$), n is the Manning bottom roughness coefficient ($\mathrm{m}^{1/3}/\mathrm{s}$), and H is water depth (m). We fix the upper limit for the Manning coefficient at 0.023 $\mathrm{m}^{1/3}/\mathrm{s}$, not exceeding the empirical maximum value in this region reported by Ni (2014).

Scenario development

We designed six numerical experiments to investigate the effects of intertidal reclamation on tidal dynamics along the Jiangsu coast (Table 1). In Case 0, the model was run using the existing condition (with all tidal flats included). In Cases 1, 2, and 3, about 35, 65, and 100% of the inshore tidal flat area were reclaimed, respectively. In Case 4, in addition to complete reclamation of the inshore tidal flat, two offshore artificial islands, covering an area of 400 km^2, were constructed. In Case 5, only 400 km^2 of the offshore tidal flat was reclaimed. These scenarios are based on the recently approved 1800 km^2 reclamation project along the Jiangsu coast and are in accordance with the engineering design of this project. Since most of the validation data were obtained in 2012, we ran the model for a year with a timestep of 5 min, from June 1, 2011, to June 1, 2012.

Tidal duration asymmetry

Tidal asymmetry refers to the difference in duration and magnitude of flood and ebb currents (Speer et al. 1991) and has a significant influence on net sediment transport in coastal areas (Postma 1961; Friedrichs and Aubrey 1988; Nidzieko 2010). According to Song et al. (2013), tidal duration asymmetry in the study area is mainly created by a combination of M_2 and M_4 tide ($2\omega_{M_2} = \omega_{M_4}$). In the following discussion, we use γ_{M_2/M_4} to evaluate the degree of tidal duration asymmetry, expressed as follows (Song et al. 2011):

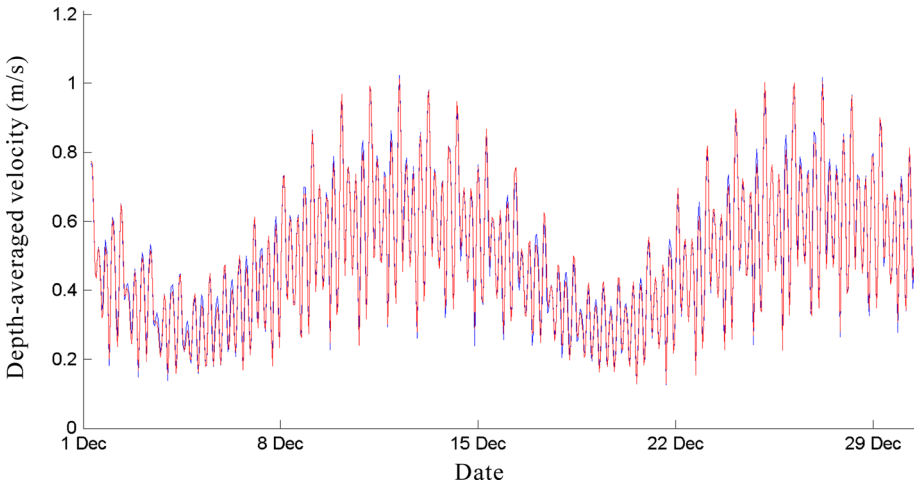

Fig. 6 Comparison of barotropic and baroclinic depth-averaged velocity at stations V1. *Red lines* represent the 3D baroclinic simulation, and *blue lines* show the 2DH barotropic simulation

Table 1 Descriptions of experiments for investigating the effects of intertidal reclamation on tidal patterns

Experiment	Description
Case 0	Reference experiment with all tidal flats included
Case 1	With 35% of inshore intertidal areas reclaimed
Case 2	With 65% of inshore intertidal areas reclaimed
Case 3	With 100% of inshore intertidal areas reclaimed
Case 4	With 100% of inshore intertidal areas and two major offshore intertidal areas reclaimed
Case 5	With two major offshore intertidal areas (total 400 km^2) reclaimed

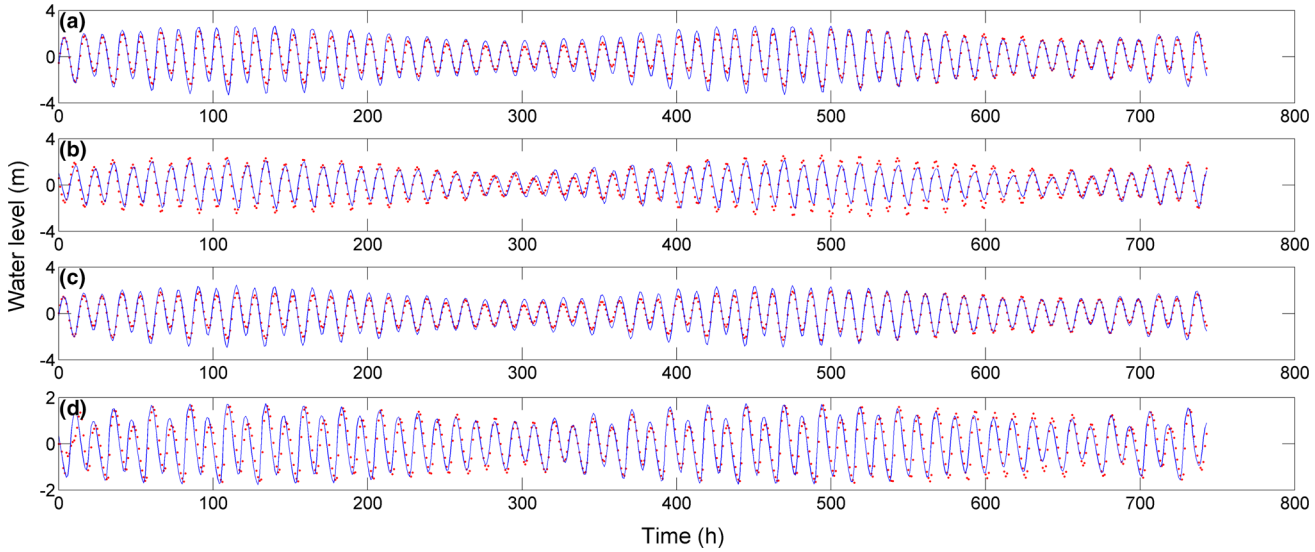

Fig. 7 Comparison of measured and modeled water levels at four coastal stations: **a** Lianyungang; **b** Lvsi; **c** Rizhao; and **d** Xinyanggang. *Red dots* represent observational data, and *blue lines* show model simulation results

$$\gamma_{M_2/M_4} = \frac{\frac{3}{2}a_{M_2}^2 a_{M_4}\sin\left(2\varphi_{M_2} - \varphi_{M_4}\right)}{\left[\frac{1}{2}\left(a_{M_2}^2 + 4a_{M_4}^2\right)\right]^{\frac{3}{2}}}, \quad (3)$$

where a_{M_2}, φ_{M_2} are the amplitudes (m) and phases (°) of the M_2 tide, respectively; a_{M_4}, φ_{M_4} are the amplitudes (m) and phases (°) of the M_4 tide, respectively. The ebb tide duration is shorter than the flood tide duration if $\gamma_{M_2/M_4} < 0$ and vice versa. In addition, $2\varphi_{M_2} - \varphi_{M_4} = 0°$ or 180° gives a distorted, but symmetric tide.

Tidal energy flux

Considering the barotropic tides and strong vertical mixing processes in the southern Yellow Sea, we use the following equation (Gill 1982) to calculate the vertically averaged tidal energy flux:

$$F = \frac{\rho g H}{T}\int \delta\vec{U}\,dt, \quad (4)$$

where F is the tidal energy flux (W/m), ρ is water density (kg/m^3), g is gravitational acceleration (m/s^2), H is water depth (m), T is the tidal period (s), δ is the water level (m), and $\vec{U}$ is the depth-averaged velocity (m/s).

Results and discussion

Model performance

The Delft3D model results were validated using water level data recorded at four coastal tide stations (Fig. 2b) from the National Marine Data and Information Service (NMDIS). The water level data, taken at hourly interval, cover a period from January 1 to February 1 in 2007. The predicted water level in our model agrees well with those data from NMDIS and has a mean deviation of <15% (Fig. 7). Comparisons of the amplitudes and phases of the main tidal constituents near Xingyanggang were also performed by tidal harmonic analysis (Table 2). The results demonstrate a solid agreement between the model and the observed data.

To further evaluate the performance of our model, the simulation results were compared with water level and current velocity data from seven anchor stations (S1–S7;

Table 2 Comparison of modeled and observed tidal harmonic parameters near Xingyanggang

Main tidal constituent	Amplitude (m)		Amplitude deviation (%)	Phase (°)		Phase deviation (°)
	Observed	Model		Observed	Model	
O_1	0.13	0.15	15.4	347.1	351.3	4.2
K_1	0.20	0.20	0.0	48.5	35.7	−12.8
N_2	0.16	0.15	−6.3	310.3	285.0	−25.3
M_2	1.23	1.26	2.4	316.6	303.1	−13.5
S_2	0.50	0.51	2.0	37.8	43.7	5.9
K_2	0.14	0.14	0.0	60.2	55.0	−5.2
M_4	0.17	0.16	−5.9	163.0	128.5	−34.5

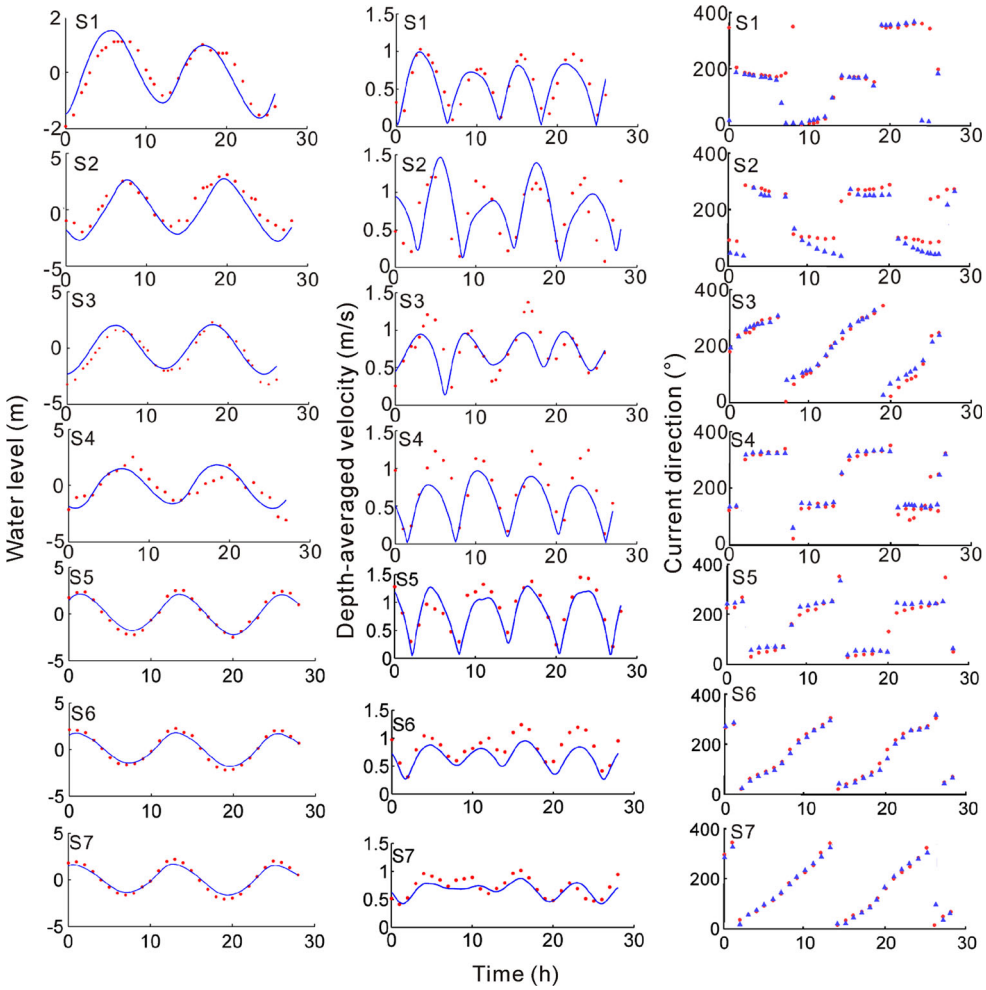

Fig. 8 Comparison of measured and modeled data including water level, depth-averaged velocity, and current direction at seven anchor stations (for locations, see Fig. 2). *Red dots* represent observational data, and *blue lines* (*blue triangles*) show model simulation results

Fig. 8), measured using an acoustic Doppler current profiler (Workhorse 600k, Teledyne RD Instruments, USA). In situ measurements were undertaken every hour at stations S1 from 17:00 on January 3 to 19:00 on January 4 in 2007, S2 from 17:00 on January 3 to 21:00 on January 4 in 2007, S3 from 6:00 on August 24 to 8:00 on August 25 in 2006, S4 from 5:00 on August 24 to 8:00 on August 25 in 2006, and S5, S6, and S7 from 12:00 on July 3 to 16:00 on July 4 in 2011. The mean deviation of the model water level from the observed data is 13.8%. The average deviation between the model current directions and the observed data is <20° among seven anchor stations. Considering the complex terrain and difficulties in field measurements in the radial sand ridge system, the discrepancy in depth-averaged velocity between observed and modeled data is acceptable, when

compared with the previous modeling studies in this region (e.g., Xing et al. 2012; Xu et al. 2016). In conclusion, the model results show reasonably good agreement with the observed values, and we believe that this model can be used to accurately simulate the tidal hydrodynamics in the study area.

Tides in the study area

Since the M_2 and S_2 tides are predominant in the southern Yellow Sea and the tidal asymmetry results mostly from a superposition of the M_2 and M_4 tides, we focus on the M_2, S_2, and M_4 tides.

As shown in Fig. 9, the coastal waters near Jiangsu are mainly controlled by the M_2 and S_2 semidiurnal tides. In both tides, there is an amphidromic point near 121.7°E, 34.6°N. The amplitude of the M_2 tide is ~2.2 m offshore from central Jiangsu, while that of the S_2 tide is ~0.8 m. These two tides contribute to a large proportion of the total tidal range in the study area. Tidal phases of the M_2 and S_2 tides demonstrate that two different tidal waves converge near the Jianggang coast. They correspond to the southern Yellow Sea rotary tidal wave and the East China Sea progressive tidal wave, respectively (Zhang 1992). The distribution of tidal amplitude and phase for the M_2 and S_2 tides agrees well with the results of Fang et al. (2004), which indicates the reliability of our model for this region.

As the first overtide of the M_2 tide, the M_4 tide is complex in this region. Its amplitude increases significantly along the central Jiangsu coast and reaches a maximum height of 0.4 m. The M_4 tidal variation is more sensitive to changes in coastline and submarine topography, especially in the shallow water of the radial sand ridge system.

Effects of reclamation on tides

Variations in the M_2 and M_4 tides

Our results indicate that if tidal flats in Jiangsu are reclaimed, the M_2 amplitude along the coast will increase significantly. As the reclamation area of inshore tidal flats increases from 35 to 100%, the amplitude of the M_2 tide correspondingly increases by 0.3 m along the coast (Fig. 10a–c). The area of the region with an enhanced M_2 amplitude also increases significantly following reclamation. The reclamation of both inshore and offshore tidal flats in Case 4 will result in the formation of an embayment-shaped zone in the north, with the amplitude of M_2 tide increasing by 0.4 m (Fig. 10d). Reclamation of offshore tidal flats in Case 5 has little influence on the M_2 amplitude (Fig. 10e). We do not present the results for the M_2 phase in these cases, as the results are similar for each case.

Generated by self-interactions of the M_2 tide, the M_4 tidal amplitude gradually increases by 0.1 m in shallow water offshore from central Jiangsu from Case 1 to Case 4 (Fig. 11a–d). A slight decrease in the M_4 tide amplitude of ~0.05 m may occur in Jianggang due to the reclamation of offshore tidal flats (Fig. 11e). Changes of the M_2 and M_4 tidal amplitude at some typical regions caused by reclamation are also shown in Table 3. Stations NR, JG, and SR denote the northern region, Jianggang, and the southern region, respectively (the location of these stations is shown in Fig. 3). Reclamation in Cases 3 and 4 results in significant increases of M_2 and M_4 tidal amplitudes in northern region. The M_4 tidal amplitude is more sensitive in southern region (variations more than 20%), while the changes in M_2 tidal amplitude are <10% there. Moreover, reclamation of offshore tidal flats in Case 5 has little influence on the M_2 and M_4 amplitudes, except for the southern region.

Tidal duration asymmetry

As mentioned in "Regional setting" section, the study area is dominated by flood currents associated with net landward sediment transport. Tidal asymmetry skewness γ_{M_2/M_4} is positive in most areas of the sand ridge system in Case 0, with a value of ~0.4–0.6 in the coastal waters off the central Jiangsu coast (Fig. 12a). Negative tidal asymmetry skewness occurred in the southern region and had a value of −0.15. Song et al. (2011) reported a similar symmetry skewness pattern near the amphidromic point.

In Case 1, when 35% of the inshore tidal flats are reclaimed the γ_{M_2/M_4} value near the coast decreases by 0.05. In Case 2 (65% inshore reclamation), inshore skewness increases by 0.05 while offshore tidal asymmetry decreases by 0.07. With 100% reclamation of inshore tidal flats in Case 3, the skewness value remains positive (0.05) along inshore coastal areas, but decreases by 0.1 offshore. With the inshore tidal flat reclamation, tidal waves will deform in shallow waters, which might enhance the inshore sediment transport in the nearshore zones. If, as in Case 4, all inshore intertidal areas and two major offshore intertidal areas are reclaimed, tidal asymmetry skewness reduces significantly by 0.2 in the southern region. This dramatic change in tidal asymmetry pattern is caused by tidal energy redistribution and topography effect following reclamation. However, if only two major offshore intertidal areas are reclaimed, the tidal asymmetry skewness γ_{M_2/M_4} remains fairly stable.

Tidal energy redistribution

Tidal energy flux in the study area indicates that tidal energy is transported into intertidal areas through tidal

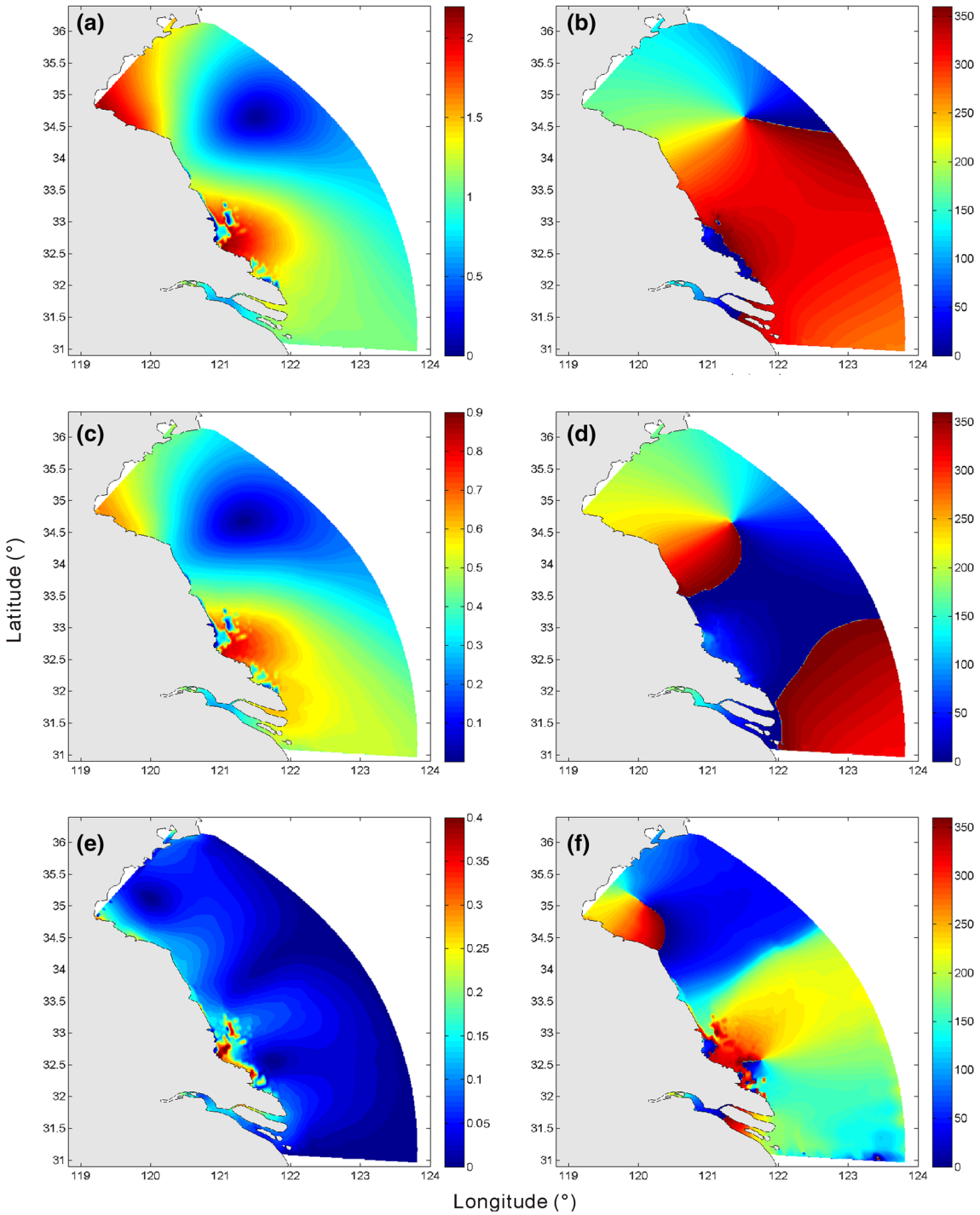

Fig. 9 Modeled amplitudes and phases of major tides: **a** amplitudes and **b** phases of the M_2 tide; **c** amplitudes and **d** phases of the S_2 tide; **e** amplitudes and **f** phases of the M_4 tide

channels. Its magnitude is about 100 kW/m in the main channels (Fig. 13a). However, the tidal energy which was originally stored and dissipated in tidal flats is transported offshore due to tidal flat reclamation. In Case 3 (Fig. 13b) where all the inshore tidal flats are reclaimed, the flux is channeled offshore with an average magnitude of 50 kW/m in the south. In Case 4, when two major offshore tidal flats and all inshore tidal flats are reclaimed, tidal energy decreases markedly in the surrounding shallow-water areas and is transported offshore through channels in the north and south, with a magnitude of 60 kW/m (Fig. 13c). In Case 5, there is no obvious change in tidal energy flux following the reclamation of two major offshore tidal flats (Fig. 13d).

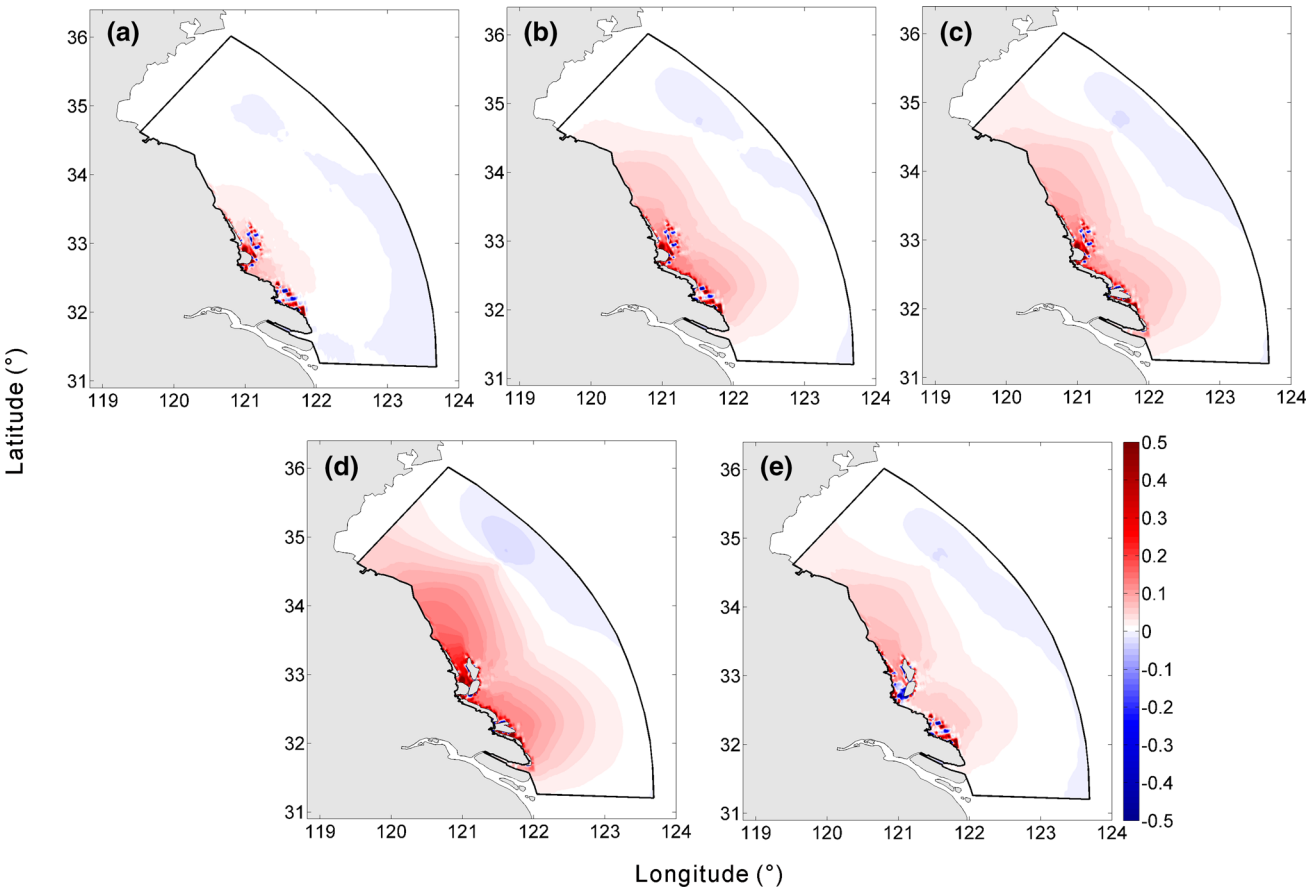

Fig. 10 Amplitude changes of the M_2 tide due to reclamation: **a** Case 1-Case 0; **b** Case 2-Case 0; **c** Case 3-Case 0; **d** Case 4-Case 0; and **e** Case 5-Case 0. The meaning of the hyphen is 'minus'

To better understand the systematic adjustment of tidal pattern, which is controlled by tidal energy distribution, we developed a conceptual model. As shown in Fig. 14, two components of tidal energy are added to the system before the reclamation of tidal flats. The red component is the energy stored and dissipated in intertidal areas, while the blue component is the energy stored elsewhere in the same system. Following land reclamation, once the intertidal areas are removed from the system the energy stored in the tidal flat has to be redistributed. A small component is dissipated and stored in other places, but remains in the system. A large portion of the remaining tidal energy released from the reclaimed tidal flats, is then transported offshore and results in far-field effects in other surrounding systems.

Potential environmental risks

Global sea-level rise has resulted in increased storm surge events and wetland losses in recent decades (Nicholls et al. 1999; Karim and Mimura 2008). Due to low coastal elevation and vast tidal flats with low slopes, the Jiangsu coast is one of the most vulnerable areas affected by sea-level rise in China. According to Yang et al. (1997), a 0.5-m sea-level rise in the southern Yellow Sea will result in the inundation of 5000 km^2 of tidal flats in Jiangsu. The results of our model indicate that tidal amplitude will increase by up to 0.4 m in this region following tidal flat reclamation of an area of 1800 km^2. This enhancement in tidal amplitudes will significantly increase the probability of low-lying coastal areas being submerged by storm surge events.

As a result, the tidal asymmetry skewness distribution in the study area changes from a flood-dominated one to a flood-dominated in the north and ebb-dominated in the south pattern, under the influence of intertidal reclamation and construction of artificial islands (Fig. 12e). These hydrodynamic differences between the north and south will lead to variability in the morphological evolution of the coast. The coast along the southern region will most likely suffer from severe erosion.

The systematic change in tidal energy pattern in the case of large-scale intertidal reclamation has not only local but also far-field effects on tidal dynamics. Our study demonstrates that intertidal reclamation can drastically change

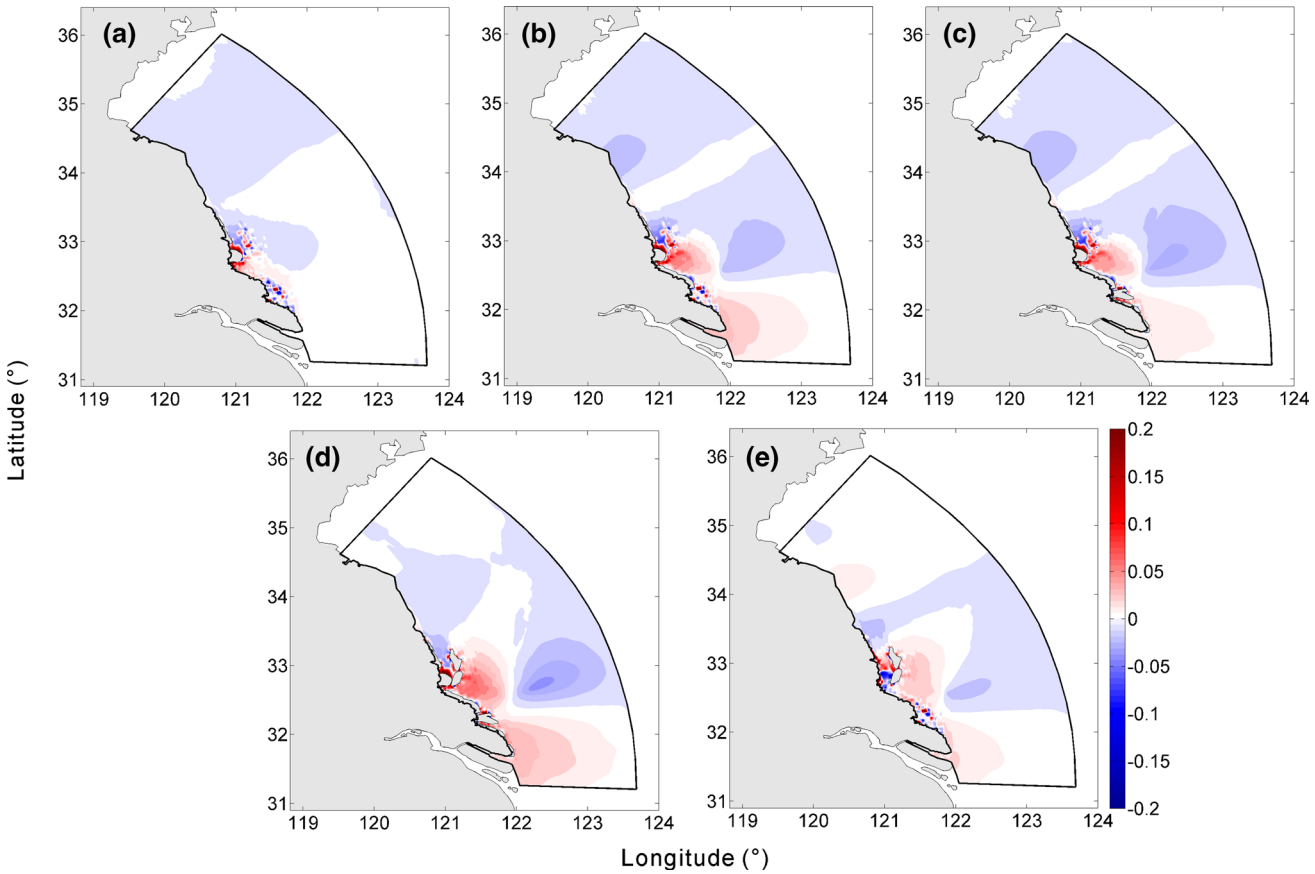

Fig. 11 Amplitude changes of the M_4 tide due to reclamation: **a** Case 1-Case 0; **b** Case 2-Case 0; **c** Case 3-Case 0; **d** Case 4-Case 0; and **e** Case 5-Case 0. The meaning of the hyphen is 'minus'

Table 3 Changes in amplitudes (%) of M_2 and M_4 tidal constitutes at some typical stations compared with Case 0

Stations	M_2			M_4		
	Case 3	Case 4	Case 5	Case 3	Case 4	Case 5
NR	16.55	24.65	2.47	26.48	33.17	9.08
JG	6.78	8.61	0.30	−1.45	0.39	−0.46
SR	5.58	8.01	3.45	22.03	49.75	33.04

local hydrodynamics, resulting in tidal energy redistribution in the southern Yellow Sea region. Song et al. (2013) studied the far-field effects of intertidal reclamation along the east China seas. They suggest that the M_2 tidal constituent has a 0.10- to 0.25-m rise in amplitude in the west Korean coastal regions after large-scale reclamation along the Jiangsu coast. On the other hand, reclamation along the west coast of Korea will change the tidal range in the Yellow Sea and the Bohai Sea (e.g., a 0.3-m rise in tidal range in Haizhou Bay). Therefore, any disturbance to tidal dynamics on either the west or east coast of the Yellow Sea might affect the entire tidal system.

Management strategies

According to the land reclamation scheme on the Jiangsu coast, inshore tidal flats with an area of 1400 km^2 and offshore tidal flats with an area of 400 km^2 will be reclaimed by 2020 (Jiangsu Development and Reform Commission and Jiangsu Coastal Areas Development Office 2009). Moreover, this scheme plans future tidal flat reclamation with an area of 2866 km^2 from 2020 to 2050 (Fig. 15). There are going to be significant environmental impacts if such a huge amount of tidal flats are reclaimed.

Therefore, it is necessary to take some measures to cope with the potential environmental risks caused by reclamation. Firstly, environmental impact assessment and overseeing of reclamation plans should be principal aspects of land reclamation management. Although all marine engineering projects in China are required to carry out an environmental impact assessment, this assessment work is often carried on only for a few months and concentrating more on environmental quality and economy resources (Chen 2009). A long-term and comprehensive environmental impact assessment has the potential to assist measures to avoid serious impacts on environment (Wang et al.

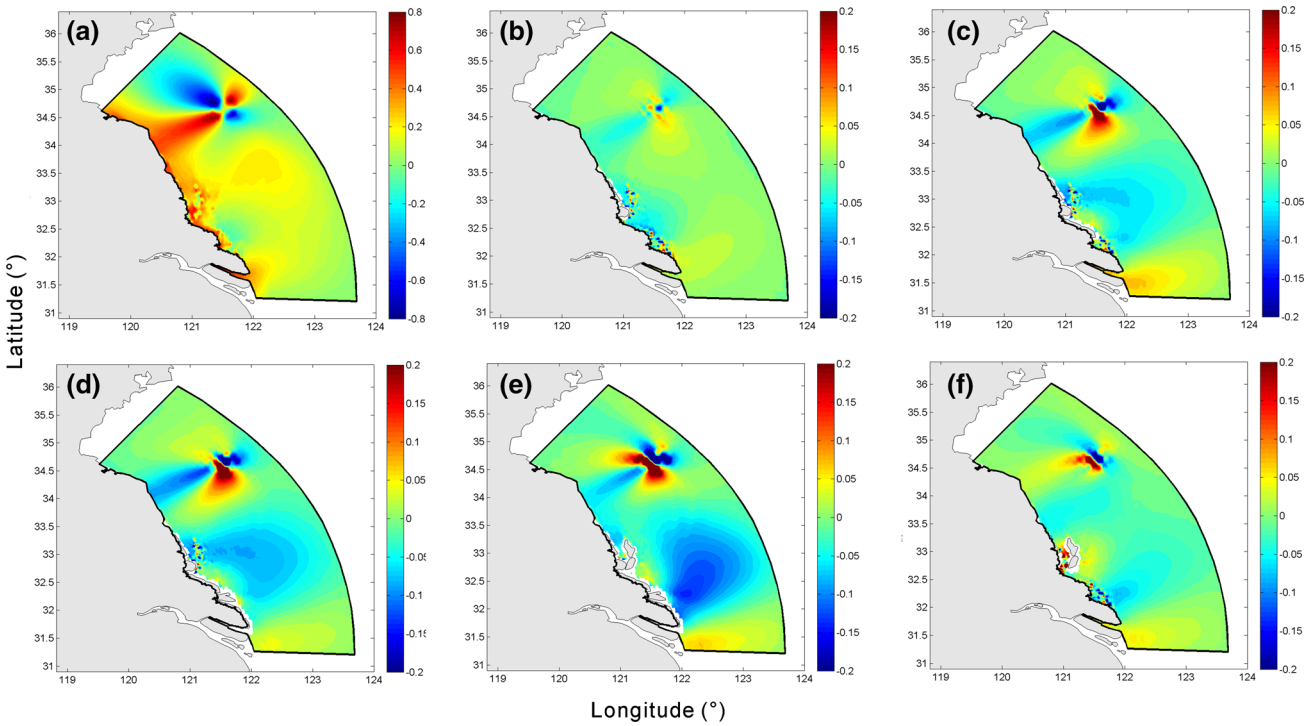

Fig. 12 Changes in tidal asymmetry skewness γ_{M_2/M_4} based on varying land reclamation simulations: **a** Case 0; **b** Case 1-Case 0; **c** Case 2-Case 0; **d** Case 3-Case 0; **e** Case 4-Case 0; and **f** Case 5-Case 0. The meaning of the hyphen is 'minus'

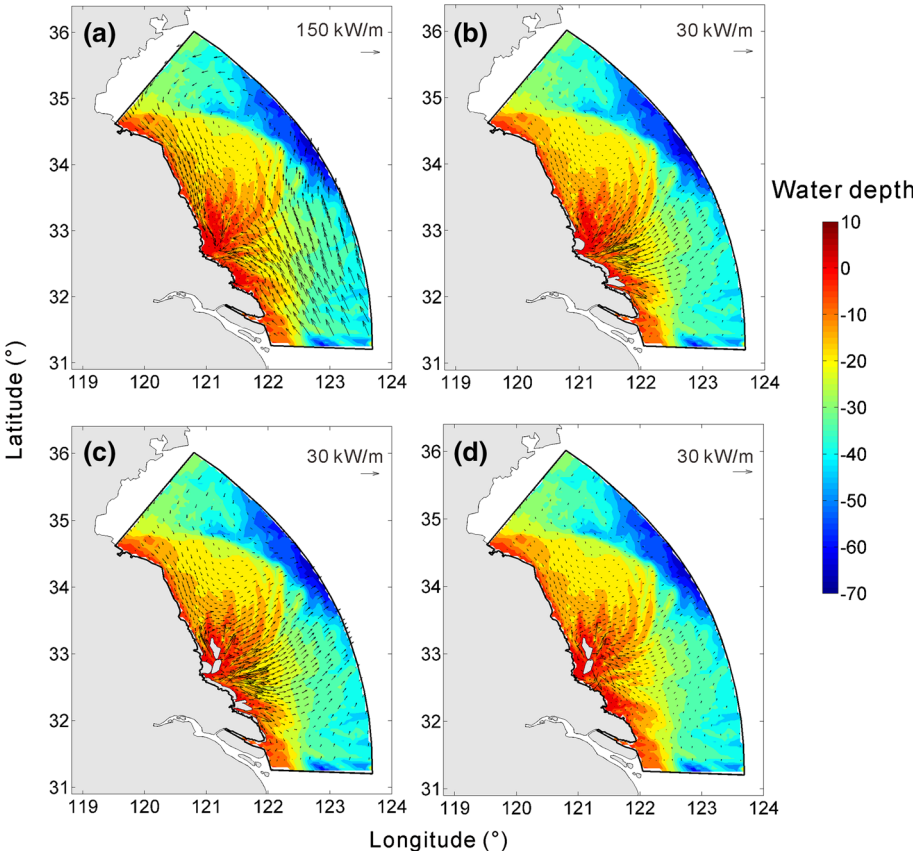

Fig. 13 Vertically averaged tidal energy flux: **a** Case 0; **b** Case 3-Case 0; **c** Case 4-Case 0; and **d** Case 5-Case 0. The meaning of the hyphen is 'minus'

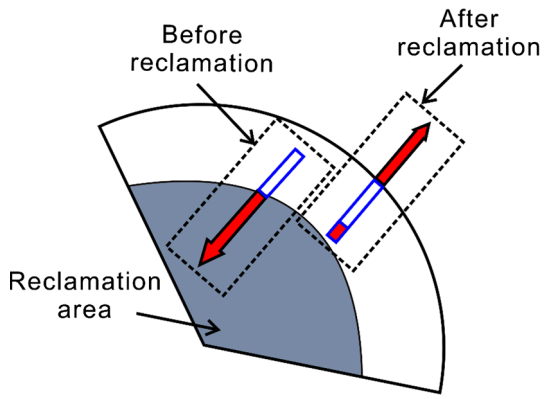

Fig. 14 Conceptual model showing tidal energy redistribution in the case of tidal flat reclamation. The *red component* is the energy stored and dissipated in intertidal areas before reclamation, and the *blue component* is the energy stored in other places in the same system

2014). Meanwhile, it is also imperative to build a coastal monitoring system to refresh the status of susceptible coastal areas and defenses. Considering the increased tidal amplitudes caused by reclamation in Jiangsu, low-lying coastal areas are probably submerged by storm surge events (Figs. 10, 11). The regions dominated by ebb currents may be highly susceptible to increased erosion (Fig. 12), thereby aggravating potential wetland losses. These vulnerable regions demand regular monitoring and protection.

In addition, international cooperation in terms of coastal management between affected countries is important to diminish these environmental impacts. In the past five decades, Korea and China have engaged in extensive coastal development and significant land reclamation as a direct result of economic growth. These disturbances have resulted in complex environmental problems in the east China seas (Song et al. 2013; Choi 2014; Wang et al. 2014). However, there is no a unified management organization to advance cooperation and meditate the potential environment risks in this region. A consensus of sustainable development via policy, legislation, science and management approaches should be reached so that contradiction between economy development and environment protection can be better resolved. As summarized by Yue et al. (2016), total quantity control and intensive management systems for land reclamation in China can be applied to a larger region, especially among the coastal countries bordering the east China seas.

Furthermore, the future of coastal development lies in offshore intertidal reclamation, which could be a possible way to alleviate increasing demands for land resources. We discussed how offshore intertidal reclamation has less influence on tidal amplitudes, tidal asymmetry, and tidal energy distribution than inshore tidal flat reclamation ("Effects of reclamation on tides" section). In other words, since the coastal system in this region appears sensitive to damage to inshore tidal flats, it would instead be desirable to reclaim offshore intertidal flats and retain the inshore flats as a buffer zone. Once the inshore tidal flats can be reserve as a marine functional zone, it is an effective way of compensation for the loss of marine ecosystem services due to reclamation.

Conclusions

A two-dimensional depth-averaged Delft3D model was used to simulate the tidal dynamics of the radial sand ridge system in the southern Yellow Sea. The model results were validated using water level data from four coastal tide stations for 1 month, as well as water level and current velocity data from seven anchor stations. The model results are in good agreement with the observed values in both magnitude and trend.

The model results show that the M_2 tide is predominant in this region, with an amplitude of 2.2 m along the central Jiangsu coast, followed by the S_2 tide with an amplitude of 0.8 m. The tidal phases of these two tides demonstrate that the southern Yellow Sea rotary tidal wave and the East China Sea progressive tidal wave converge near the Jianggang coast. The M_4 tide, the first overtide of the M_2 tide, is complex in this region and has a maximum amplitude of 0.4 m.

Six numerical experiments were performed to investigate the effects of intertidal reclamation on tides along the Jiangsu coast. The results demonstrate that tidal flats are critical modulators of tidal dynamics in this region. The reclamation of both inshore and offshore tidal flats will result in three remarkable changes in tidal patterns: enhanced M_2 and M_4 tidal amplitudes in coastal areas with increments of 0.4 and 0.1 m, respectively; strengthened negative tidal asymmetry skewness in the southern region of the sand ridge system; and an enhanced flux, with a magnitude of 60 kW/m, transporting tidal energy offshore through the main channels in the south. Reclamation of just 400 km^2 of offshore tidal flats has a smaller influence on tidal amplitudes, tidal asymmetry, and tidal energy distribution as compared with inshore reclamation.

The potential risks of hydrodynamic changes in the southern Yellow Sea, caused by reclamation, include increased tidal amplitude and offshore sediment transport along the southern Jiangsu coast. The former may enhance the probability of coastal hazards (e.g., low-lying coastal areas being frequently submerged during storm surge events) and the latter may result in severe erosion, threatening the safety of coastal facilities. The enhanced energy flux transporting offshore might also result in far-field

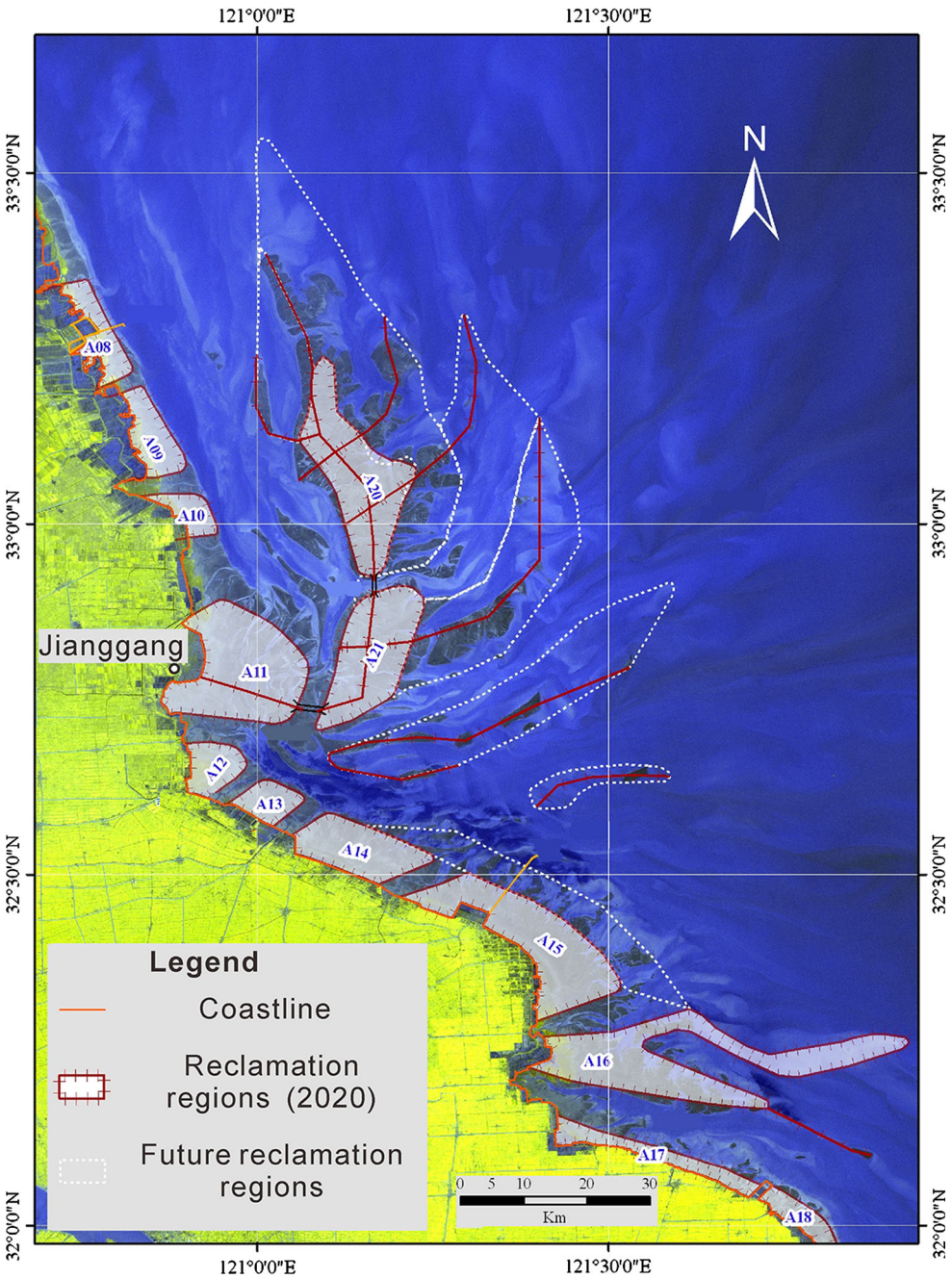

Fig. 15 Map showing land reclamation scheme on the Jiangsu coast

effects along other coastal systems bordering the southern Yellow Sea.

To cope with the potential environmental risks caused by reclamation, it is recommended to strengthen environmental impact assessment and overseeing of reclamation plans, advance international cooperation in terms of coastal management, and reclaim offshore intertidal flats while retaining the inshore flats as a buffer zone.

Acknowledgements Financial supports for the study were provided by the Major State Basic Research Development Program (2013CB956502), the Natural Science Foundation of China (Nos. 41376044 and 41625021), Geological environment investigation and evaluation on Jiangsu Coastal Economic Zone project issued by China Geological Survey (No. 1212011220005), and the PAPD of Jiangsu Higher Education Institutions. Prof. X. Wang (UNSW) is thanked for his comments on an early version of the text.

References

Apotsos A, Jaffe B, Gelfenbaum G (2011) Wave characteristic and morphologic effects on the onshore hydrodynamic response of tsunamis. Coast Eng 58(11):1034–1048

Bao X, Gao G, Yan J (2001) Three dimensional simulation of tide and tidal current characteristics in the East China Sea. Oceanol Acta 24(2):135–149

Camorani G, Castellarin A, Brath A (2005) Effects of land-use changes on the hydrologic response of reclamation systems. Phys Chem Earth Parts A/B/C 30(8):561–574

Chen SQ (2009) On strengthening the environmental management of China's reclamation projects (in Chinese). Ocean Dev Manag 26(9):22–26 (**in Chinese**)

Chen K, Jiao JJ (2008) Metal concentrations and mobility in marine sediment and groundwater in coastal reclamation areas: a case study in Shenzhen, China. Environ Pollut 151(3):576–584

Cho D-O (2007) The evolution and resolution of conflicts on Saemangeum Reclamation Project. Ocean Coast Manag 50(11–12):930–944

Choi YR (2014) Modernization, development and underdevelopment: reclamation of Korean tidal flats, 1950s–2000s. Ocean Coast Manag 102:426–436

Edmonds DA, Slingerland RL (2007) Mechanics of river mouth bar formation: implications for the morphodynamics of delta distributary networks. J Geophys Res Earth Surf. doi:10.1029/2006JF000574

Ertürk ŞN, Bilgili A, Swift MR, Brown WS, Çelikkol B, Ip JTC et al (2002) Simulation of the Great Bay Estuarine System: tides with tidal flats wetting and drying. J Geophys Res Oceans 107(C5):61–610

Fang G (1986) Tide and tidal current charts for the marginal seas adjacent to China. Chin J Oceanol Limnol 4(1):1–16

Fang G, Wang Y, Wei Z, Choi BH, Wang X, Wang J (2004) Empirical cotidal charts of the Bohai, Yellow, and East China Seas from 10 years of TOPEX/Poseidon altimetry. J Geophys Res Oceans 109(C11):1–13

Fernández S, Santín C, Marquínez J, Álvarez MA (2010) Saltmarsh soil evolution after land reclamation in Atlantic estuaries (Bay of Biscay, North coast of Spain). Geomorphology 114(4):497–507

Friedrichs CT, Aubrey DG (1988) Non-linear tidal distortion in shallow well-mixed estuaries: a synthesis. Estuar Coast Shelf Sci 27(5):521–545

Gill A (1982) Atmosphere-ocean dynamics. In: Adrian EG (ed) International geophysics, vol 30. Academic Press, San Diego, p 662

Guo X, Yanagi T (1998) Three-dimensional structure of tidal current in the East China Sea and the Yellow Sea. J Oceanogr 54(6):651–668

Hu K, Ding P, Wang Z, Yang S (2009) A 2D/3D hydrodynamic and sediment transport model for the Yangtze Estuary, China. J Mar Syst 77(1):114–136

Jiangsu Development and Reform Commission, Jiangsu Coastal Areas Development Office (2009) Development program guidelines for Jiangsu coastal inter-intertidal reclamation and exploitation (Government document). http://govinfo.nlc.gov.cn/jssfz/jszb/201020/201104/t20110414_696110.shtml?classid=416

Jiao J, Wang X, Nandy S (2006) Preliminary assessment of the impacts of deep foundations and land reclamation on groundwater flow in a coastal area in Hong Kong, China. Hydrogeol J 14(1–2):100–114

Kang JW (1999) Changes in tidal characteristics as a result of the construction of sea-dike/sea-walls in the Mokpo Coastal Zone in Korea. Estuar Coast Shelf Sci 48(4):429–438

Kang SK, Lee S-R, Lie H-J (1998) Fine grid tidal modeling of the Yellow and East China Seas. Cont Shelf Res 18(7):739–772

Karim MF, Mimura N (2008) Impacts of climate change and sea-level rise on cyclonic storm surge floods in Bangladesh. Glob Environ Change 18(3):490–500

Larsen L, Cannon G, Choi B (1985) East China Sea tide currents. Cont Shelf Res 4(1):77–103

Leonardi N, Canestrelli A, Sun T, Fagherazzi S (2013) Effect of tides on mouth bar morphology and hydrodynamics. J Geophys Res Oceans 118(9):4169–4183

Lesser GR, Roelvink JA, van Kester JATM, Stelling GS (2004) Development and validation of a three-dimensional morphological model. Coast Eng 51(8):883–915

Li L, Wang XH, Williams D, Sidhu H, Song D (2012) Numerical study of the effects of mangrove areas and tidal flats on tides: a case study of Darwin Harbour, Australia. J Geophys Res Oceans 117(C6):1–12. doi:10.1029/2011JC007494

Li L, Wang XH, Andutta F, Williams D (2014) Effects of mangroves and tidal flats on suspended-sediment dynamics: observational and numerical study of Darwin Harbour, Australia. J Geophys Res Oceans 119(9):5854–5873

Liu Z, Huang Y, Zhang Q (1989) Tidal current ridges in the southwestern Yellow Sea. J Sediment Res 59(3):432–437

Naser HA (2011) Effects of reclamation on macrobenthic assemblages in the coastline of the Arabian Gulf: a microcosm experimental approach. Mar Pollut Bull 62(3):520–524

Ni W (2014) Numerical simulation on the geomorphodynamics of tidal channel-sand ridge-tidal flat system in the southern Yellow Sea. Master thesis, Nanjing University

Nicholls RJ, Hoozemans FMJ, Marchand M (1999) Increasing flood risk and wetland losses due to global sea-level rise: regional and global analyses. Glob Environ Change 9(Supplement 1):S69–S87

Nidzieko NJ (2010) Tidal asymmetry in estuaries with mixed semidiurnal/diurnal tides. J Geophys Res Oceans. doi:10.1029/2009JC005864

Nidzieko NJ, Ralston DK (2012) Tidal asymmetry and velocity skew over tidal flats and shallow channels within a macrotidal river delta. J Geophys Res Oceans. doi:10.1029/2011JC007384

Nishida H (1980) Improved tidal charts for the western part of the North Pacific Ocean. Rep Hydrogr Res 15:55–70

Postma H (1961) Transport and accumulation of suspended matter in the Dutch Wadden Sea. Neth J Sea Res 1(1–2):148–180

Ralston DK, Geyer WR, Traykovski PA, Nidzieko NJ (2013) Effects of estuarine and fluvial processes on sediment transport over deltaic tidal flats. Cont Shelf Res 60(Supplement):S40–S57

Ren ME (1986) Modern sedimentation in the coastal and nearshore zones of China. China Ocean Press, Beijing

Song D, Wang XH, Kiss AE, Bao X (2011) The contribution to tidal asymmetry by different combinations of tidal constituents. J Geophys Res Oceans. doi:10.1029/2011JC007270

Song D, Wang XH, Zhu X, Bao X (2013) Modeling studies of the far-field effects of tidal flat reclamation on tidal dynamics in the East China Seas. Estuar Coast Shelf Sci 133:147–160

Speer PE, Aubrey DG, Friedrichs CT (1991) Nonlinear hydrodynamics of shallow tidal inlet/bay systems. In: Parker BB (ed) Tidal hydrodynamics. Wiley, New York, pp 319–339

Storlazzi C, Elias E, Field M, Presto M (2011) Numerical modeling of the impact of sea-level rise on fringing coral reef hydrodynamics and sediment transport. Coral Reefs 30(1):83–96

Wang X, Ke X (1997) Grain-size characteristics of the extant tidal flat sediments along the Jiangsu coast, China. Sediment Geol 112(1–2):105–122

Wang Z, Li L, Chen D, Xu K, Wei T, Gao J, Zhao Y, Chen Z, Masabate W (2007) Plume front and suspended sediment dispersal off the Yangtze (Changjiang) River mouth, China during non-flood season. Estuar Coast Shelf Sci 71(1–2):60–67

Wang Y, Zhang Y, Zou X, Zhu D, Piper D (2012a) The sand ridge field of the Southern Yellow Sea: origin by river–sea interaction. Mar Geol 291:132–146

Wang YP, Gao S, Jia J, Thompson CEL, Gao J, Yang Y (2012b) Sediment transport over an accretional intertidal flat with influences of reclamation, Jiangsu coast, China. Mar Geol 291–294:147–161

Wang W, Liu H, Li Y, Su J (2014) Development and management of land reclamation in China. Ocean Coast Manag 102:415–425

Whitney MM, Garvine RW (2005) Wind influence on a coastal buoyant outflow. J Geophys Res Oceans. doi:10.1029/2003JC002261

Xing F, Wang YP, Wang HV (2012) Tidal hydrodynamics and fine-grained sediment transport on the radial sand ridge system in the southern Yellow Sea. Mar Geol 291:192–210

Xu F, Tao J, Zhou Z, Coco G, Zhang C (2016) Mechanisms underlying the regional morphological differences between the northern and southern radial sand ridges along the Jiangsu Coast, China. Mar Geol 371:1–17

Yang G, Shi Y, Ji Z (1997) Relative sea level rise and its unfavorable impacts in Jiangsu Coastal Plain. J Nat Disaster 6(1):88–96

Yue Q, Zhao M, Yu H, Xu W, Ou L (2016) Total quantity control and intensive management system for reclamation in China. Ocean Coast Manag 120:64–69

Zhang R (1992) Suspended sediment transport processes on tidal mud flat in Jiangsu Province, China. Estuar Coast Shelf Sci 35(3):225–233

Zhang C (2011) The general report of coastal investigation and assessment (Mission 908) in Jiangsu Province (in Chinese). Science Press, Beijing

Zhang J, Lu X, Wang P, Wang YP (2011) Study on linear and nonlinear bottom friction parameterizations for regional tidal models using data assimilation. Cont Shelf Res 31(6):555–573

Zhang X, Yan C, Pan XU, Dai Y, Yan W, Ding X et al (2013) Historical evolution of tidal flat reclamation in the Jiangsu coastal areas. Acta Geogr Sin 68(11):1549–1558

Zhu XM, Liu GM (2012) Numerical study on the tidal currents, tidal energy fluxes and dissipation in the China Seas. Oceanol Limnol Sin 43(3):669–677